

New absolute magnitude calibrations for detached binaries

S. Bilir^{1,*}, T. Ak^{1,2}, E. Soydugan³, F. Soydugan³, E. Yaz¹, N. Filiz Ak⁴, Z. Eker^{2,3}, O. Demircan³, and M. Helvacı⁵

¹ Istanbul University, Faculty of Sciences, Department of Astronomy and Space Sciences, 34119 Istanbul, Turkey

² TÜBİTAK National Observatory, Akdeniz University Campus, 07058 Antalya, Turkey

³ Çanakkale Onsekiz Mart University, Faculty of Sciences and Arts, Department of Physics, 17100 Çanakkale, Turkey

⁴ Erciyes University, Faculty of Sciences and Arts, Department of Astronomy and Space Sciences, Talas Yolu, 38039 Kayseri, Turkey

⁵ Ankara University, Faculty of Sciences, Department of Astronomy and Space Sciences, 06100 Ankara, Turkey

The dates of receipt and acceptance should be inserted later

Key words stars: distances, (stars:) binaries: eclipsing

Lutz-Kelker bias corrected absolute magnitude calibrations for the detached binary systems with main-sequence components are presented. The absolute magnitudes of the calibrator stars were derived at intrinsic colours of Johnson-Cousins and 2MASS (Two Micron All Sky Survey) photometric systems. As for the calibrator stars, 44 detached binaries were selected from the *Hipparcos* catalogue, which have relative observed parallax errors smaller than 15% ($\sigma_\pi/\pi \leq 0.15$). The calibration equations which provide the corrected absolute magnitude for optical and near-infrared pass bands are valid for wide ranges of colours and absolute magnitudes: $-0.18 < (B - V)_0 < 0.91$, $-1.6 < M_V < 5.5$ and $-0.15 < (J - H)_0 < 0.50$, $-0.02 < (H - K_s)_0 < 0.13$, $0 < M_J < 4$, respectively. The distances computed using the luminosity-colours (LCs) relation with optical (BV) and near-infrared (JHK_s) observations were compared to the distances found from various other methods. The results show that new absolute magnitude calibrations of this study can be used as a convenient statistical tool to estimate the true distances of detached binaries out of *Hipparcos*' distance limit.

© 2008 WILEY-VCH Verlag GmbH & Co. KGaA, Weinheim

1 Introduction

The most reliable physical parameters of stars, e.g. masses, radii, effective temperatures etc., used in testing theoretical predictions of fundamental physical structure of single stars, are obtained from the observations of detached eclipsing binaries with main-sequence components. Masses and radii could be determined within an accuracy better than 1% from their light and radial velocity curves (Andersen, 1991; Southworth et al., 2004, 2005a).

There could be several techniques to determine distances for detached eclipsing binaries. The most reliable distances are usually the ones from accurately measured trigonometric parallaxes or interferometric observations of nearby stars. Relatively less reliable distances are the ones based on spectroscopic or photometric parallaxes using absolute magnitudes estimated or computed from the solutions of data obtained by photometric or spectroscopic observations. Such distances, however, require measurements of reliable reddening free apparent magnitudes. The effect of interstellar reddening on the final distance predictions could be larger than expected. Since reddening is less effective at infrared wavelengths, the prediction errors could be minimized by using infrared photometry (Southworth et al., 2005b).

Relation between orbital period, luminosity and colours of the binary stars, called PLC relation, was first proposed by Rucinski (1974) (see also, Mochnacki, 1981) for W UMa-type binaries in order to reduce the scatter in the main-sequence colour-magnitude relation. Rucinski (1994) established the PLC relation of W UMa-type stars using $(B - V)$, $(V - I_c)$ colours and orbital periods. The PLC relation of W UMa-type binaries was improved later using *Hipparcos* parallaxes (Rucinski & Duerbeck, 1997). In a recent paper, Ak et al. (2007) described a similar relation, called PLCs relation for cataclysmic binaries. Although it is possible to find a PLCs relation for detached binaries too, applying this idea to detached binaries makes no sense since the orbital period is not correlated in any physical way to the components. Thus, a relation between the luminosity (absolute magnitude) and colours can be more useful for detached binaries. It should be noted that more accurate calibrations can be obtained by using two colours instead of one colour, since one colour dependent calibrations may include systematic errors (see, e.g. Bilir et al., 2008).

In this study, we first estimate the systemic V and J band absolute magnitudes M_V and M_J of detached binaries using reliable trigonometric parallaxes from *Hipparcos* satellite by assuming that the light in V and J bands comes from the system as a *whole*. Then, we find the dependence of the absolute magnitude on de-reddened colours $(B - V)_0$, $(J - H)_0$ and $(H - K_s)_0$ to derive absolute magnitude cali-

* Corresponding author: e-mail: sbilir@istanbul.edu.tr

brations for detached binaries with observations in Johnson-Cousins and 2MASS photometric systems. We should state that our aim is *not* to measure the absolute magnitudes of each component in the detached binaries in our list.

Unfortunately, measured parallaxes are never free from systematic errors. This problem has been noticed by Lutz & Kelker (LK, 1973). Assuming uniform spatial distribution of stars and a uniform distribution of observed parallaxes around the true parallax, LK explained that there must be a systematic error, known as Lutz-Kelker bias, in computed distances which depends only upon relative parallax error (σ_π/π), where π is observed parallax and σ_π is the associated standard error. Because of LK bias, the true parallaxes are always smaller than observed parallaxes (Lutz & Kelker, 1973). Therefore observed parallaxes are needed to be corrected. This correction procedure is recognized as LK correction.

According to Jerzykiewicz (2001), only the studies which are careful to use parallaxes with $(\sigma_\pi/\pi) \leq 0.1$ could be excused since the bias could be tolerable. Otherwise, LK bias (if not corrected) would either alter conclusions or invalidate the results. However, the standard LK corrections become significant if $(\sigma_\pi/\pi) \geq 0.05$ and increase as relative error gets bigger (Maiz Apellániz, 2005). Thus the parallaxes with such significant errors must be corrected.

Aim of this study is to establish an absolute magnitude calibration for practical usage to estimate distances of detached main-sequence eclipsing binaries which have no trigonometric parallax nor known physical structures to imply their absolute brightness, but only have at least an eclipsing light curve indicating they are on the main sequence and detached. Unlike the common practice of predicting binary distances photometrically, which requires estimated absolute magnitudes of each component extracted from the light contributions of each component and/or their physical parameters from a spectroscopic or a light curve solution, this new method does not require extensive work; thus practical and quick, therefore, useful especially when studying large numbers of eclipsing data such as ASAS (Paczyński et al., 2006) survey where light curve solutions are not available to most binaries.

2 The Data

Photometric data of 44 detached eclipsing binaries with main-sequence components, which have observed trigonometric parallaxes (π) with relative errors smaller than $(\sigma_\pi/\pi) \leq 0.15$, were collected from the literature. The 14 of them are chromospherically active binaries taken from Eker et al. (2008). Since there are relative errors of the observed parallaxes bigger than 0.05, LK correction needs to be applied to derive the true parallaxes (π_0) using following equation (Smith, 1987):

$$\pi_0 = \pi \left(\frac{1}{2} + \frac{1}{2} \sqrt{1 - 16(\sigma_\pi/\pi)^2} \right). \quad (1)$$

Table 1 contains the basic data required for absolute magnitude calibration. The columns are organized as order,

name, spectral type, galactic coordinates (ℓ, b), observed parallaxes (π), relative parallax error (σ_π/π), LK corrected true parallaxes (π_0), colour excess ($E(B-V)$), visual brightness (V) and colour ($B-V$), infrared brightness (J) and colours ($J-H, H-K_s$) and quality flag. Quality flag "AAA" indicates the best quality or maximum reliability of 2MASS photometric data.

Parallaxes, parallax errors, galactic coordinates and J, H and K_s magnitudes are taken from the *Hipparcos* catalogue (ESA, 1997) and the Point-Source Catalogue and Atlas (Cutri et al., 2003) which is based on the 2MASS (Two Micron All Sky Survey) observations, respectively, by using VizieR¹ service. The 2MASS photometric system comprises Johnson's J (1.25 μm) and H (1.65 μm) bands with the addition of K_s (2.17 μm) band, which is bluer than Johnson's K -band (Skrutskie et al., 2006). Spectral types were collected from the available literature.

2.1 Intrinsic colours and absolute magnitudes

In principle, a calibration in any photometric system has to be based on the intrinsic (de-reddened) colours, such as $(B-V)_o, (J-H)_o$ and $(H-K_s)_o$. However, unlike the observed colours, the intrinsic colours require one more step to be estimated from any kinds of colour excess values if spectroscopic observations are not available to reveal them independently. For estimating the intrinsic colours, the colour excess of $E(B-V)$ has been preferred for this study. Unfortunately, only limited number of $E(B-V)$ colour excesses of some systems were given in the literature. Therefore, we used Schlegel et al. (1998) maps and NASA Extragalactic Database² to calculate the $E(B-V)$ value of a star. Schlegel et al. (1998) maps provide only the $E(B-V)$ values according to galactic coordinates, which are the modeled values for any direction from Sun to the edges of our Galaxy as a consequence of the galactic dust. The colour excess values according to galactic latitude (b) and longitude (ℓ) towards the directions of stars are shown by $E_\infty(B-V)$, which symbolically means up to infinity but actually up to the edge of the Galaxy. Therefore, the $E_\infty(B-V)$ values have to be reduced according to the actual distance of each star. The total interstellar absorption within the Galaxy in the photometric V band was computed from an available modeled value of $E_\infty(B-V)$ for a given galactic latitude (b) as

$$A_\infty(b) = 3.1E_\infty(B-V). \quad (2)$$

The total interstellar absorption in the V band up to the distance ($d = 1/\pi$) of the star can be estimated by (Bahcall & Soneira, 1980)

$$A_d(b) = A_\infty(b) \left[1 - \exp\left(-\frac{|d \sin(b)|}{H}\right) \right], \quad (3)$$

¹ <http://vizier.u-strasbg.fr/viz-bin/VizieR>

² <http://nedwww.ipac.caltech.edu/forms/calculator.html>

where H is the scaleheight for the interstellar dust which is adopted as 125 pc (Marshall et al., 2006). Finally, the colour excess for a star at the distance d is estimated from

$$E_d(B - V) = A_d(b) / 3.1. \quad (4)$$

Once we obtained the colour excess for a star, we have calculated the intrinsic magnitudes and colours as following: $V_o = V - 3.1 \times E_d(B - V)$, $(B - V)_o = (B - V) - E_d(B - V)$, $J_o = J - 0.887 \times E_d(B - V)$, $(J - H)_o = (J - H) - 0.322 \times E_d(B - V)$, $(H - K_s)_o = (H - K_s) - 0.183 \times E_d(B - V)$. We used the equations of Fiorucci & Munari (2003) (see also, Bilir, Güver & Aslan, 2006) for the determination of the total absorption for J band and colour excesses of $(J - H)$ and $(H - K_s)$ colours. All the magnitudes and colours with subscript “0” will be mentioned as de-reddened ones, hereafter.

In addition to intrinsic magnitudes and colours, fundamental input data required for the calibration are absolute magnitudes. The absolute magnitude of stars in Table 1 have been computed by the well known distance-modulus formula both for optical and near-infrared bands, i.e. $M_{V_{LK}} = V_o - 5 \log(1/\pi_0) + 5$ and $M_{J_{LK}} = J_o - 5 \log(1/\pi_0) + 5$, respectively. The computed values of M_V and M_J are given in columns 3 and 5 in Table 2. Corresponding propagated errors were calculated as $\delta M = 2.17(\sigma_\pi/\pi) + \delta m$, where (σ_π/π) and δm are relative parallax error and the error of the apparent magnitude in the relevant photometric system, respectively.

3 Absolute magnitude calibrations

Selected colours and LK corrected absolute magnitudes M_V and M_J according to *Hipparcos* distances for the sample stars (Tables 1 and 2) were used in calibrating the coefficients of the following equations:

$$M_V = a(B - V)_o + c, \quad (5)$$

$$M_J = a(J - H)_o + b(H - K_s)_o + c. \quad (6)$$

The coefficients of each equation and their 1σ errors have been determined by the method of least squares. All 44 systems in Table 1 were used to predict the coefficients for the relation using optical colour (Eq. 5). However, only 37 out of 44 were used in the calibrations involving 2MASS data since observed colours with the quality flag “AAA” were preferred for them. The predicted coefficients and their uncertainties together with the correlation coefficients, standard deviations and standard errors are given in Table 3. Consequently, it can be concluded that each equation above would provide an absolute magnitude with an internal uncertainty of ± 0.09 mag. Moreover, since the correlation coefficients are 0.91 and 0.95 (Table 3), strong correlations between the involved parameters (absolute magnitude and colours) are confirmed. The calibrated equations can be considered valid within the ranges $-0.18 < (B - V)_o < 0.91$ and $-1.6 < M_V < 5.5$ for the calibration including optical colour, and $-0.15 < (J - H)_o < 0.50$, $-0.02 <$

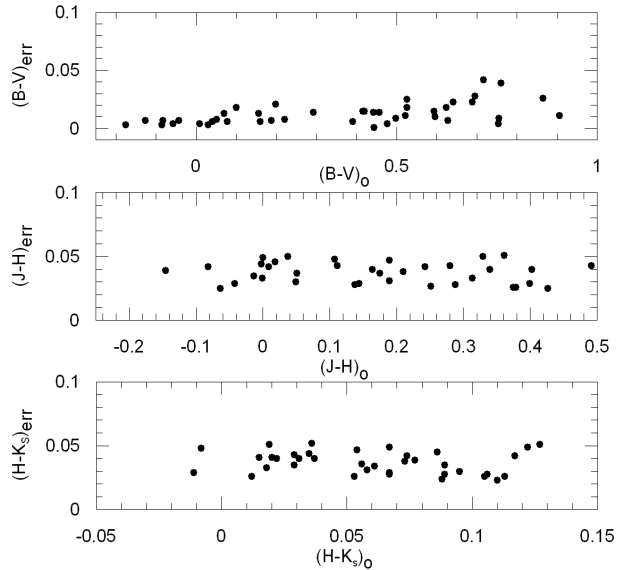


Fig. 1 Colour errors for the optical and 2MASS data.

$(H - K_s)_o < 0.13$ and $0 < M_J < 4$ for the 2MASS photometric system. These limits correspond to the spectral classes $B4 - K7$ (Covey et al., 2007; Cox, 2000). The calibrations are based on the trigonometric parallaxes with the relative errors $(\sigma_\pi/\pi) \leq 0.15$.

3.1 Uncertainties of the calibrations

In order to see how accurate the observed colours are, the errors of the observed colours have been plotted against the intrinsic colours in Fig. 1 where the visual colour $((B - V)_0)$ have smaller uncertainties than the near-infrared colours $((J - H)_0, (H - K_s)_0)$. The mean observational errors are about 0.02 ($\sigma = \pm 0.02$) and 0.04 ($\sigma = \pm 0.01$) mag in the optical and near-infrared colours, respectively. This is not surprising, because 2MASS magnitudes were obtained from single-epoch observations, while optical observations have been done more than once. These mean errors of colours introduce typically ± 0.17 and ± 0.22 mag uncertainties at M_V and M_J , respectively.

Uncertainty in the de-reddening introduces an additional uncertainty. Due to smaller de-reddening at infrared colours, infrared calibrations are expected to be less affected by de-reddening process.

Some of the binaries can be unrecognized as triple or multiple systems. Thus, their parallax measurements cannot be reliable. Assuming that the parallaxes of systems in our sample are precise enough, a median (σ_π/π) value of 0.07 of the sample introduces a typical error of ± 0.15 mag.

3.2 Comparison with *Hipparcos* absolute magnitudes and distances

Absolute magnitudes predicted by LCs relations are compared to the absolute magnitudes obtained from *Hipparcos* catalogue for the calibration stars (Fig. 2). Almost all

Table 1 The data used in calibration of the absolute magnitudes. π_0 shows LK corrected parallax. “Quality” denotes the quality flag of 2MASS data.

ID	Star	Spectral type	ℓ ($^{\circ}$)	b ($^{\circ}$)	π (mas)	(σ_{π}/π)	π_0 (mas)	$E_d(B-V)$ (mag)	V (mag)	$(B-V)$ (mag)	J (mag)	$(J-H)$ (mag)	$(H-K_s)$ (mag)	Quality
1	RT And	G0V + K2V	108.058	-6.926	13.26	0.09	12.87	0.020 ^a	8.97 \pm 0.017	0.546 \pm 0.018	8.037 \pm 0.018	0.257 \pm 0.027	0.093 \pm 0.028	AAA
2	V805 Aql	A2 + A7	24.163	-8.544	5.80	0.15	5.22	0.130 ^b	7.60 \pm 0.010	0.286 \pm 0.013	6.970 \pm 0.027	0.079 \pm 0.050	0.078 \pm 0.047	AAA
3	β Aur	A1V + A1V	167.457	10.409	39.72	0.02	39.66	0.000 ^c	1.90 \pm 0.005	0.077 \pm 0.006	1.756 \pm 0.222	-0.004 \pm 0.278	-0.018 \pm 0.254	DCC
4	AR Aur	B9V + B9.6V	172.768	-2.233	8.20	0.10	7.89	0.000 ^d	6.15 \pm 0.007	-0.043 \pm 0.007	6.190 \pm 0.019	-0.064 \pm 0.025	-0.011 \pm 0.029	AAA
5	WW Aur	A4m + A5m	181.724	10.519	11.86	0.09	11.47	0.000 ^e	5.82 \pm 0.005	0.188 \pm 0.007	5.498 \pm 0.021	-0.001 \pm 0.033	0.018 \pm 0.033	AAA
6	ZZ Boo	F3V + F3V	31.820	75.482	8.88	0.09	8.60	0.012 ^f	6.78 \pm 0.005	0.402 \pm 0.006	5.982 \pm 0.021	0.115 \pm 0.043	0.037 \pm 0.044	AAA
7	SV Cam	F9V + K4V	131.572	26.523	11.77	0.09	11.37	0.015 ^g	9.30 \pm 0.019	0.703 \pm 0.023	7.872 \pm 0.023	0.366 \pm 0.051	0.130 \pm 0.051	AAA
8	AR Cas	B4V + A6V	112.466	-2.659	5.67	0.10	5.44	0.054 ^f	4.89 \pm 0.003	-0.122 \pm 0.003	5.092 \pm 0.023	-0.035 \pm 0.054	-0.037 \pm 0.055	EAA
9	YZ Cas	A1Vm + F2V	122.549	12.121	11.24	0.05	11.13	0.070 ^g	5.64 \pm 0.003	0.078 \pm 0.004	5.585 \pm 0.019	-0.059 \pm 0.042	0.042 \pm 0.043	AAA
10	V636 Cen	G0V + G7V	316.742	10.619	15.36	0.07	15.03	0.027 ^h	8.67 \pm 0.015	0.650 \pm 0.018	7.474 \pm 0.030	0.348 \pm 0.040	0.066 \pm 0.034	AAA
11	EK Cep	A2V + G5Vp	107.724	12.653	6.53	0.09	6.32	0.000 ⁱ	7.88 \pm 0.011	0.069 \pm 0.013	7.632 \pm 0.026	0.051 \pm 0.037	0.022 \pm 0.040	AAA
12	RS Cha	A8V + A8V	292.551	-21.632	10.23	0.04	10.15	0.031 ^a	6.05 \pm 0.015	0.229 \pm 0.021	5.994 \pm 0.030	0.117 \pm 0.048	0.025 \pm 0.051	AAA
13	RZ Cha	F5V + F5V	298.410	-20.324	5.43	0.12	5.12	0.004 ^h	8.05 \pm 0.011	0.460 \pm 0.014	7.131 \pm 0.030	0.190 \pm 0.047	0.037 \pm 0.052	AAA
14	WY Cne	G5V + K9V	199.471	39.307	11.76	0.15	10.65	0.011 ^a	9.49 \pm 0.034	0.727 \pm 0.042	7.992 \pm 0.023	0.403 \pm 0.029	0.108 \pm 0.028	AAA
15	α CrB	A0V + G5V	41.870	53.772	43.65	0.02	43.59	0.007 ^a	2.22 \pm 0.003	0.032 \pm 0.003	2.249 \pm 0.242	-0.145 \pm 0.315	0.188 \pm 0.415	DCD
16	V1143 Cyg	F5V + F5V	87.251	15.595	25.12	0.02	25.07	0.005 ^j	5.89 \pm 0.003	0.482 \pm 0.004	4.979 \pm 0.020	0.139 \pm 0.028	0.068 \pm 0.028	AAA
17	DE Dra	B9V + G2V	96.483	14.364	8.62	0.06	8.49	0.040 ^a	5.71 \pm 0.003	-0.043 \pm 0.007	5.695 \pm 0.021	-0.029 \pm 0.029	0.019 \pm 0.026	AAA
18	TX Her	A5V + F0V	66.872	34.440	5.55	0.15	4.99	0.000 ^k	8.11 \pm 0.010	0.292 \pm 0.014	7.535 \pm 0.023	0.049 \pm 0.030	0.095 \pm 0.030	AAA
19	V624 Her	A3Vm + A7V:	38.716	21.250	6.93	0.11	6.60	0.051 ^l	6.18 \pm 0.005	0.211 \pm 0.006	5.740 \pm 0.019	0.034 \pm 0.026	0.056 \pm 0.018	AAF
20	V772 Her	G0V + G5V	47.757	19.298	26.51	0.05	26.23	0.026 ^h	7.07 \pm 0.006	0.654 \pm 0.007	5.818 \pm 0.030	0.337 \pm 0.050	0.127 \pm 0.049	AAA
21	HS Hya	F4V + F4V	261.349	31.676	11.04	0.08	10.75	0.024 ^a	8.08 \pm 0.012	0.466 \pm 0.014	7.206 \pm 0.021	0.172 \pm 0.040	0.077 \pm 0.038	AAA
22	KW Hya	A5Vm + F0V	237.548	26.953	12.10	0.07	11.85	0.012 ^m	6.10 \pm 0.005	0.232 \pm 0.008	5.654 \pm 0.023	0.022 \pm 0.046	0.088 \pm 0.045	AAA
23	GZ Leo	K1V + K1V	217.241	64.826	18.43	0.06	18.11	0.007 ^a	8.96 \pm 0.019	0.872 \pm 0.026	7.244 \pm 0.019	0.428 \pm 0.025	0.111 \pm 0.023	AAA
24	UV Leo	G0V + G2V	228.700	56.462	10.85	0.11	10.33	0.016 ^a	8.91 \pm 0.019	0.657 \pm 0.023	8.069 \pm 0.026	0.318 \pm 0.033	0.108 \pm 0.026	AAA
25	UW LMi	F8V + F8V	202.219	61.777	7.73	0.14	7.07	0.003 ^c	8.34 \pm 0.012	0.596 \pm 0.015	7.320 \pm 0.034	0.281 \pm 0.043	0.059 \pm 0.031	AAA
26	GG Lup	B7V + B9V	330.846	13.954	6.34	0.11	5.99	0.027 ⁿ	5.59 \pm 0.005	-0.099 \pm 0.007	6.117 \pm 0.020	-0.137 \pm 0.039	0.042 \pm 0.040	AAA
27	FL Lyr	F8V + G8V	77.268	15.933	7.69	0.12	7.25	0.049 ^o	9.35 \pm 0.022	0.574 \pm 0.025	8.243 \pm 0.026	0.258 \pm 0.042	0.086 \pm 0.039	AAA
28	V478 Lyr	G8V + M2V	61.852	10.124	35.70	0.02	35.63	0.008 ^a	7.78 \pm 0.007	0.763 \pm 0.009	6.232 \pm 0.020	0.377 \pm 0.026	0.114 \pm 0.026	AAA
29	TZ Men	B9V + G1V	297.348	-28.827	9.35	0.05	9.24	0.055 ^a	6.18 \pm 0.004	-0.003 \pm 0.004	6.137 \pm 0.029	0.018 \pm 0.049	0.002 \pm 0.048	AAA
30	UX Men	F8V + F8V	287.845	-31.096	9.93	0.06	9.77	0.027 ^p	8.23 \pm 0.010	0.549 \pm 0.011	7.195 \pm 0.027	0.219 \pm 0.038	0.061 \pm 0.036	AAA
31	η Mus	B8V + B9V	305.178	-5.127	8.04	0.07	7.86	0.008 ^q	4.79 \pm 0.002	-0.078 \pm 0.003	4.949 \pm 0.044	-0.082 \pm 0.050	0.040 \pm 0.033	EAA
32	EE Peg	A3mV + F5V	64.182	-31.117	7.61	0.12	7.14	0.020 ^a	6.96 \pm 0.015	0.120 \pm 0.018	6.720 \pm 0.018	0.003 \pm 0.044	0.071 \pm 0.049	AAA
33	V505 Per	F5V + F5V	135.812	-6.101	15.00	0.06	14.81	0.012 ^a	6.86 \pm 0.007	0.456 \pm 0.001	6.070 \pm 0.067	0.277 \pm 0.076	0.022 \pm 0.041	AAA
34	V570 Per	F5V + F5V	145.178	-8.189	8.53	0.11	8.07	0.071 ^a	8.05 \pm 0.012	0.491 \pm 0.015	7.160 \pm 0.026	0.212 \pm 0.031	0.066 \pm 0.026	AAA
35	ζ Phe	B6V + B8V	297.833	-61.714	11.66	0.07	11.45	0.000 ^r	3.94 \pm 0.004	-0.120 \pm 0.020	4.216 \pm 0.450	0.001 \pm 0.570	0.011 \pm 0.539	DDD
36	UV Psc	G5V + K3V	134.149	-55.504	15.87	0.08	15.42	0.017 ^a	8.98 \pm 0.023	0.712 \pm 0.028	7.633 \pm 0.029	0.407 \pm 0.040	0.092 \pm 0.035	AAA
37	BB Scl	K3V + K4V	231.697	-80.036	42.29	0.03	42.08	0.003 ^s	7.11 \pm 0.009	0.909 \pm 0.011	5.340 \pm 0.023	0.367 \pm 0.079	0.283 \pm 0.078	AEA
38	CD Tau	F6V + F6V	183.955	-10.136	13.66	0.12	12.82	0.026 ^h	6.69 \pm 0.009	0.523 \pm 0.009	5.851 \pm 0.021	0.183 \pm 0.037	0.079 \pm 0.042	AAA
39	V818 Tau	G6V + K6V	177.621	-23.356	21.40	0.06	21.11	0.005 ^a	8.32 \pm 0.017	0.756 \pm 0.004	6.865 \pm 0.020	0.379 \pm 0.026	0.089 \pm 0.024	AAA
40	V1229 Tau	A0Vp + Am	166.535	-23.319	9.05	0.11	8.61	0.025 ^t	6.83 \pm 0.011	0.066 \pm 0.006	6.635 \pm 0.023	-0.006 \pm 0.035	0.034 \pm 0.035	AAA
41	XY UMa	G9V + K7V	162.720	41.675	15.09	0.10	14.49	0.005 ^a	9.50 \pm 0.029	0.765 \pm 0.039	7.770 \pm 0.020	0.493 \pm 0.043	0.118 \pm 0.042	AAA
42	PT Vel	A1V + A6V	266.180	3.329	6.20	0.10	5.94	0.004 ^u	7.02 \pm 0.006	0.055 \pm 0.008	6.863 \pm 0.030	0.010 \pm 0.042	0.016 \pm 0.041	AAA
43	ER Vul	G0V + G5V	73.342	-12.306	20.06	0.04	19.92	0.018 ^h	7.33 \pm 0.007	0.614 \pm 0.010	6.082 \pm 0.019	0.294 \pm 0.028	0.070 \pm 0.029	AAA
44	HD 71636	F2V + F5V	184.980	34.803	8.54	0.11	8.10	0.026 ^h	7.88 \pm 0.010	0.441 \pm 0.015	7.074 \pm 0.020	0.152 \pm 0.029	0.036 \pm 0.040	AAA

calibration stars are located in the prediction limits of 2σ . Fig. 2 and Table 3 show that absolute magnitudes calculated from the calibration equation using near-infrared colours have stronger correlation and less scatter on diagonal. The distances predicted from the distance modulus have been compared in a similar manner in Fig. 3. Standard deviations of the residuals from the *Hipparcos* distances are 37 and 26 pc for optical and near infrared colours, respectively. These values show that the calibration equation including near-infrared colours are better in correlation as expected than the absolute magnitude comparisons given above. In Fig. 3a-b, we showed the 1σ prediction limits. Systems located out of 1σ prediction limits are indicated. It is interesting to note that these scattered systems are almost the same as in Fig. 3a-b.

The distances predicted from the distance modulus have been compared in a similar manner in Fig. 3. Standard deviations of the residuals from the *Hipparcos* distances are 37 and 26 pc for optical and near infrared colours, respectively. These values show that the calibration equation including near-infrared colours are better in correlation as expected than the absolute magnitude comparisons given above. In Fig. 3a-b, we showed the 1σ prediction limits. Systems located out of 1σ prediction limits are indicated. It is interesting to note that these scattered systems are almost the same as in Fig. 3a-b.

Table 3 Least square coefficients of Eqs. 5-6. R , s and se denote correlation coefficient, standard deviation and standard error, respectively.

Eq.	a	b	c	R	s	se
5	5.908(\pm 0.309)	—	0.204(\pm 0.143)	0.95	0.63	0.09
6	5.228(\pm 0.715)	6.185(\pm 3.173)	0.608(\pm 0.154)	0.91	0.49	0.08

4 Application to the other detached systems

In order to compare the distances estimated from our calibrations and various methods, 48 detached systems other than our sample with main-sequence components and known distances were collected from the literature. Among these stars, distances of 16 systems were taken from the *Hipparcos* catalogue with $0.15 < (\sigma_{\pi}/\pi) \leq 0.5$. For the rest of stars, distances were found from photometric analysis.

Table 2 Absolute magnitudes and distances calculated from LK corrected *Hipparcos* parallaxes and Eqs. 5-6 for 44 detached binaries.

ID	Star	Hip	Eq. 5	Hip	Eq. 6	Hip	Hip	Eq. 5	Eq. 6
		$M_{V_{LK}}$	M_V	$M_{J_{LK}}$	M_J	d (pc)	d_{LK} (pc)	d (pc)	d (pc)
1	RT And	4.456±0.201	3.312±0.125	3.567±0.202	2.471±0.153	75±6	78±6	132±7	129±6
2	V805 Aql	0.785±0.336	1.126±0.113	0.443±0.353	1.135±0.204	172±26	192±26	164±8	139±8
3	β Aur	-0.108±0.048	0.659±0.101	—	—	25±1	25±1	18±1	—
4	AR Aur	0.635±0.213	-0.050±0.104	0.675±0.225	0.205±0.153	122±12	127±12	174±9	157±9
5	WW Aur	1.118±0.198	1.315±0.102	0.796±0.214	0.714±0.167	84±8	87±8	80±4	91±4
6	ZZ Boo	1.415±0.196	2.508±0.101	0.643±0.212	1.405±0.188	113±10	116±10	70±4	82±4
7	SV Cam	4.533±0.216	4.269±0.132	3.138±0.220	3.281±0.205	85±8	88±8	99±6	82±5
8	AR Cas	-1.599±0.218	-0.836±0.096	—	—	176±18	184±18	129±7	—
9	YZ Cas	0.655±0.109	0.251±0.097	0.755±0.125	0.359±0.184	89±4	90±4	108±6	108±5
10	V636 Cen	4.471±0.173	3.885±0.123	3.335±0.188	2.758±0.184	65±5	67±5	87±5	87±5
11	EK Cep	1.884±0.204	0.612±0.114	1.636±0.219	1.011±0.183	153±14	158±14	284±15	211±12
12	RS Cha	0.986±0.113	1.374±0.126	0.999±0.128	1.285±0.209	98±4	99±4	82±5	86±5
13	RZ Cha	1.584±0.263	2.898±0.115	0.673±0.282	1.819±0.209	184±22	195±22	107±5	115±7
14	WY Cnc	4.593±0.351	4.434±0.166	3.119±0.340	3.350±0.160	85±13	94±13	101±6	84±5
15	α CrB	0.395±0.042	0.352±0.096	—	—	23±1	23±1	23±2	—
16	V1143 Cyg	2.871±0.051	3.022±0.097	1.971±0.068	1.739±0.156	40±1	40±1	37±2	44±3
17	DE Dra	0.231±0.133	-0.286±0.100	0.305±0.151	0.463±0.156	116±7	118±7	149±8	109±6
18	TX Her	1.601±0.338	1.929±0.114	1.026±0.351	1.452±0.163	180±28	200±28	172±9	165±8
19	V624 Her	0.120±0.237	1.149±0.101	—	—	144±16	152±16	94±5	—
20	V772 Her	4.083±0.117	3.914±0.103	2.889±0.141	3.083±0.209	38±2	38±2	41±2	35±2
21	HS Hya	3.163±0.186	2.815±0.116	2.342±0.195	1.917±0.179	91±7	93±7	109±6	113±6
22	KW Hya	1.432±0.159	1.504±0.103	1.012±0.177	1.234±0.194	83±6	84±6	82±4	76±4
23	GZ Leo	5.228±0.160	5.314±0.135	3.528±0.160	3.515±0.147	54±4	55±4	53±3	56±2
24	UV Leo	3.931±0.251	3.991±0.132	3.126±0.258	2.894±0.165	92±10	97±10	94±5	108±6
25	UW LMi	2.578±0.316	3.707±0.117	1.564±0.338	2.431±0.188	129±18	141±18	84±5	95±5
26	GG Lup	-0.607±0.252	-0.540±0.102	-0.020±0.267	0.074±0.179	158±18	167±18	162±8	160±8
27	FL Lyr	3.500±0.274	3.306±0.137	2.502±0.278	2.349±0.187	130±15	138±15	151±9	148±8
28	V478 Lyr	5.514±0.055	4.665±0.106	3.984±0.068	3.262±0.152	28±1	28±1	41±3	39±2
29	TZ Men	0.838±0.119	-0.139±0.098	0.916±0.144	0.559±0.206	107±6	108±6	170±8	128±7
30	UX Men	3.095±0.145	3.288±0.111	2.120±0.162	2.052±0.181	101±6	102±6	94±5	106±5
31	η Mus	-0.758±0.160	-0.304±0.095	—	—	124±9	127±9	103±5	—
32	EE Peg	1.166±0.275	0.795±0.123	0.970±0.278	1.007±0.191	131±16	140±16	166±9	138±7
33	V505 Per	2.676±0.123	2.827±0.092	1.912±0.189	2.159±0.264	67±4	68±4	63±3	60±5
34	V570 Per	2.364±0.257	2.685±0.117	1.631±0.271	1.924±0.163	117±13	124±13	107±6	108±6
35	ζ Phe	-0.766±0.147	-0.505±0.314	—	—	86±6	87±6	77±4	—
36	UV Psc	4.867±0.203	4.310±0.141	3.558±0.209	3.260±0.184	63±5	65±5	84±5	74±5
37	BB Scl	5.221±0.085	5.557±0.110	—	—	24±1	24±1	20±1	—
38	CD Tau	2.148±0.268	3.140±0.107	1.367±0.281	1.981±0.180	73±9	78±9	49±3	59±3
39	V818 Tau	4.927±0.143	4.641±0.111	3.483±0.146	3.123±0.150	47±3	47±3	54±3	56±3
40	V1229 Tau	1.428±0.243	0.446±0.107	1.288±0.255	0.714±0.173	110±12	116±12	183±9	151±8
41	XY UMa	5.290±0.242	4.694±0.158	3.571±0.233	3.899±0.185	66±7	69±7	91±5	59±3
42	PT Vel	0.877±0.223	0.505±0.104	0.728±0.247	0.748±0.193	161±16	168±16	200±10	167±9
43	ER Vul	3.770±0.098	3.725±0.107	2.562±0.110	2.528±0.156	50±2	50±2	51±3	51±3
44	HD 71636	2.341±0.249	2.656±0.115	1.593±0.259	1.553±0.169	117±13	123±13	107±5	126±6

Colours, colour excesses, absolute magnitudes and distances of the selected systems are listed in Table 4. Optical and near-infrared colours of these stars were taken from *Hipparcos* catalogue (ESA, 1997) and 2MASS Point-Source Catalogue (Cutri et al., 2003), respectively. $E(B-V)$ values were either taken from the literature or calculated from Schlegel (1998) maps (see Section 2.1).

The M_V and M_J absolute magnitudes of the binaries in Table 4 (columns 9-10) were estimated from Eqs. 5 and 6,

respectively. These absolute magnitudes were used to calculate the distances by the Pogson's relation and recorded in next columns. The systems with known hypothetical third body or apsidal motion are indicated in column 14, as well.

The distances predicted from our LCs relations are compared to the distances used in literature, where various methods including trigonometric parallaxes were preferred (Fig. 4). At first glance, it looks like that predicted and collected distances are very much in agreement. Standard deviations

Table 4 Detached systems with main sequence components and known distances collected from the literature. The last column of the table gives references including information for colour excess, distance given in literature and remarks, in order.

ID Star	<i>V</i>	$(B - V)$	<i>J</i>	$(J - H)$	$(H - K_s)$	$E(B - V)$	Eq. 5		Eq. 6		Literature	
							M_V	M_J	d (pc)	d (pc)	d (pc)	Rem*
1 KZ And	7.91	0.900	6.225	0.437	0.129	0.010	5.462	3.662	30±2	32±3	25±5	(01, 02, -)
2 KP Aql	9.40	0.446	8.521	0.067	0.050	0.130	2.071	0.900	243±12	317±26	282±12	(03, 03, -)
3 V432 Aur	8.01	0.566	6.864	0.277	0.069	0.000	3.548	2.483	78±5	75±6	118±23	(04, 02, -)
4 AD Boo	9.45	0.521	8.389	0.232	0.051	0.000	3.282	2.136	171±9	178±15	203±8	(03, 03, -)
5 CV Boo	10.75	0.726	9.570	0.288	0.081	0.014	4.410	2.570	182±11	250±20	235±24	(01, 05, -)
6 AS Cam	8.59	-0.008	8.524	-0.022	0.007	0.080	-0.316	0.308	539±28	426±42	480±48	T, A (06, 07, 08)
7 WW Cam	10.16	0.510	9.182	0.065	0.081	0.397	0.872	0.334	409±21	500±39	376±12	A (09, 09, 10)
8 V392 Car	9.48	0.191	9.053	0.080	0.037	0.101	0.736	0.971	485±28	397±34	349±28	(11, 11, -)
9 IT Cas	11.15	0.488	10.212	0.255	0.042	0.062	2.721	2.028	444±13	422±34	504±26	A (12, 12, 10)
10 PV Cas	9.75	0.171	9.324	-0.017	0.046	0.217	-0.068	0.196	675±34	613±51	670±67	A (13, 13, 25)
11 SZ Cen	8.52	0.305	8.346	0.127	0.065	0.060	1.651	1.507	217±13	228±22	262±101	(14, 02, -)
12 EY Cep	9.80	0.367	9.035	0.058	0.136	0.049	2.083	1.613	326±17	299±29	307±14	A (15, 15, 10)
13 ZZ Cep	8.63	0.285	8.148	0.124	0.021	0.148	1.013	0.968	270±14	257±30	168±89	(01, 02, -)
14 TV Cet	8.61	0.439	7.753	0.131	0.073	0.067	2.402	1.555	158±10	169±16	160±7	T, A (01, 16, 08)
15 XY Cet	8.74	0.280	8.212	0.018	0.079	0.100	1.267	0.912	271±19	277±25	212±76	(17, 02, -)
16 GZ CMa	7.97	0.159	7.613	0.002	0.052	0.063	0.771	0.761	251±15	229±21	270±86	(18, 02, -)
17 MY Cyg	8.31	0.377	7.692	0.115	0.055	0.055	2.106	1.393	161±9	178±21	264±64	A (19, 02, 10)
18 V442 Cyg	9.71	0.496	9.154	0.174	0.032	0.080	2.662	1.487	229±11	331±25	317±18	(20, 03, -)
19 V477 Cyg	8.51	0.168	8.099	0.023	0.017	0.040	0.960	0.722	306±18	294±23	205±15	T, A (21, 21, 08)
20 V909 Cyg	9.56	0.141	9.180	0.017	0.064	0.066	0.647	0.909	552±27	439±35	447±28	T (03, 03, 41)
21 V1061 Cyg	9.24	0.592	8.122	0.205	0.086	0.296	1.953	1.381	188±11	198±16	167±6	T (01, 22, 22)
22 MR Del	8.77	0.696	7.033	0.481	0.143	0.013	4.239	3.974	79±5	41±3	44±11	T (01, 02, 42)
23 BS Dra	9.13	0.443	8.268	0.198	0.043	0.102	2.219	1.619	208±14	205±17	208±33	(01, 02, -)
24 UZ Dra	9.59	0.512	8.616	0.190	0.054	0.024	3.087	1.869	193±11	221±18	185±12	(03, 03, -)
25 CW Eri	8.40	0.389	7.799	0.140	0.033	0.011	2.437	1.511	153±9	180±17	168±37	(23, 02, -)
26 RX Her	7.26	0.054	7.256	0.015	-0.007	0.042	0.275	0.520	235±13	219±20	230±56	A (24, 02, 25)
27 VZ Hya	8.98	0.455	8.076	0.224	0.068	0.016	2.798	2.155	168±11	152±13	199±57	(01, 02, -)
28 CM Lac	8.20	0.190	7.843	0.018	0.057	0.060	0.972	0.887	256±14	240±27	227±45	(26, 02, -)
29 RW Lac	10.63	0.661	9.299	0.338	0.090	0.068	3.707	2.742	220±10	199±16	190±10	A (27, 27, 10)
30 TX Leo	5.67	0.059	5.515	0.012	0.061	0.016	0.458	1.003	108±5	79±8	142±20	(01, 02, -)
31 FS Mon	9.60	0.388	8.826	0.175	-0.005	0.039	2.266	1.381	277±12	303±30	321±14	(03, 03, -)
32 WZ Oph	9.10	0.551	8.574	0.205	0.100	0.032	3.270	2.209	140±8	185±18	125±22	(01, 02, -)
33 V451 Oph	7.89	0.050	7.626	-0.011	0.064	0.155	-0.416	0.512	367±20	249±29	300±30	A (28, 28, 25)
34 EW Ori	9.94	0.612	8.808	0.204	0.106	0.014	3.737	2.285	171±11	201±24	180±5	A (29, 29, 10)
35 GG Ori	10.37	0.511	9.465	0.142	0.111	0.411	0.795	0.883	457±24	440±37	430±15	A (01, 03, 10)
36 BK Peg	9.99	0.540	8.892	0.249	0.032	0.050	3.099	1.968	222±11	238±19	260±26	(30, 30, -)
37 OO Peg	8.26	0.270	7.676	0.043	0.078	0.070	1.386	1.115	214±14	199±18	295±17	(01, 31, -)
38 IQ Per	7.73	0.041	7.561	-0.030	0.047	0.140	-0.381	0.352	343±19	261±25	275±15	A (32, 32, 25)
39 PV Pup	7.03	0.345	6.574	0.155	0.015	0.010	2.183	1.483	92±5	104±9	83±5	A (01, 33, 10)
40 VV Pyx	6.57	0.043	6.403	-0.007	0.036	0.022	0.328	0.733	172±9	135±11	195±10	A (34, 34, 25)
41 AL Scl	6.09	-0.093	6.253	-0.055	0.018	0.027	-0.505	0.354	201±10	150±13	200±27	(35, 35, -)
42 QX Ser	8.68	0.635	7.477	0.266	0.098	0.054	3.637	2.454	94±5	99±9	95±10	(23, 23, -)
43 V526 Sgr	9.84	0.179	9.539	0.057	0.040	0.140	0.434	0.764	623±33	537±47	540±23	A (36, 36, 25)
44 V1647 Sgr	6.92	0.125	6.912	-0.016	0.041	0.041	0.706	0.667	165±9	175±18	160±10	A (37, 37, 25)
45 ZZ UMa	9.84	0.586	8.713	0.301	0.078	0.008	3.619	2.642	173±9	163±14	172±21	(38, 38, -)
46 BH Vir	9.65	0.650	8.459	0.274	0.113	0.035	3.837	2.645	138±10	143±18	126±25	(39, 02, -)
47 DM Vir	8.74	0.469	7.792	0.181	0.083	0.023	2.839	2.006	147±9	142±16	192±4	(40, 40, -)
48 Hip 56132	9.87	0.669	8.650	0.345	0.074	0.011	4.091	2.836	141±5	145±11	92±15	(01, 02, -)

(*) (T) Triple, (A) Apsidal motion

(**) (1) Schlegel et al. (1998), (2) ESA (1997), (3) Lacy (2002), (4) Siviero et al. (2004), (5) Nelson (2004), (6) Maloney et al. (1989), (7) Khodykin et al. (1997), (8) Bozkurt & Değirmenci (2007), (9) Lacy et al. (2002), (10) Bulut & Demircan (2007), (11) Debernardi et al. (2001), (12) Lacy et al. (1997), (13) Barembaum & Etzel (1995), (14) Andersen (1975), (15) Lacy et al. (2006), (16) Jorgensen (1979), (17) Srivastava (1987), (18) Popper et al. (1985), (19) Popper & Etzel (1981), (20) Lacy & Frueh (1987), (21) Değirmenci et al. (2003), (22) Torres et al. (2006), (23) Nordström et al. (2004), (24) Lacy (1979), (25) Petrova & Orlov (1999), (26) Popper (1968), (27) Lacy et al. (2005), (28) Clausen et al. (1986), (29) Popper et al. (1986), (30) Demircan et al. (1994), (31) Munari et al. (2001), (32) Lacy & Frueh (1985), (33) Vaz & Andersen (1984), (34) Andersen et al. (1984), (35) Haefner et al. (1987), (36) Lacy (1997a), (37) Andersen & Gimenez (1985), (38) Clement et al. (1997a), (39) Clement et al. (1997b), (40) Latham et al. (1996), (41) Lacy (1997b), (42) Cutispoto et al. (1997)

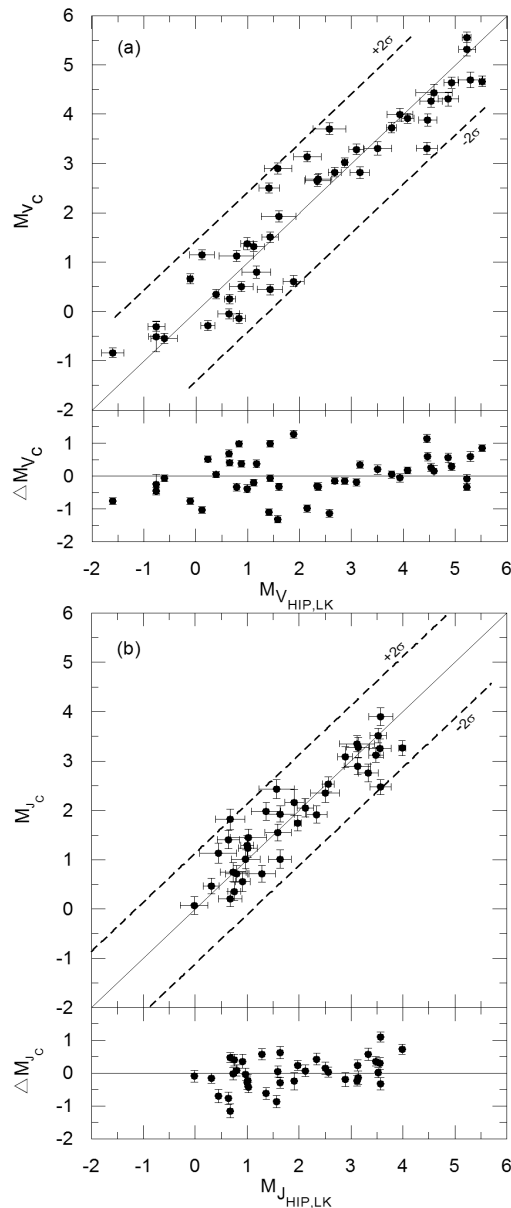


Fig. 2 Absolute magnitudes predicted by the Eqs. 5 (a) and 6 (b) versus visual and near-infrared absolute magnitudes calculated from LK corrected *Hipparcos* parallaxes.

of the residual distances are ~ 50 pc for both the calibration equations using optical and near infrared colours. The systems with distances higher than ~ 400 pc have the largest scatter. However, an eye inspection shows that scatter even for these distant systems is not higher than ~ 100 pc, indicating a precision better than $\sim 25\%$. In fact, the scatter in Fig. 4 are mostly due to uncertainties in distance measurements in the literature (particularly those from uncertain *Hipparcos* parallaxes), so the scatter in the calibrations should be smaller than the overall scatter.

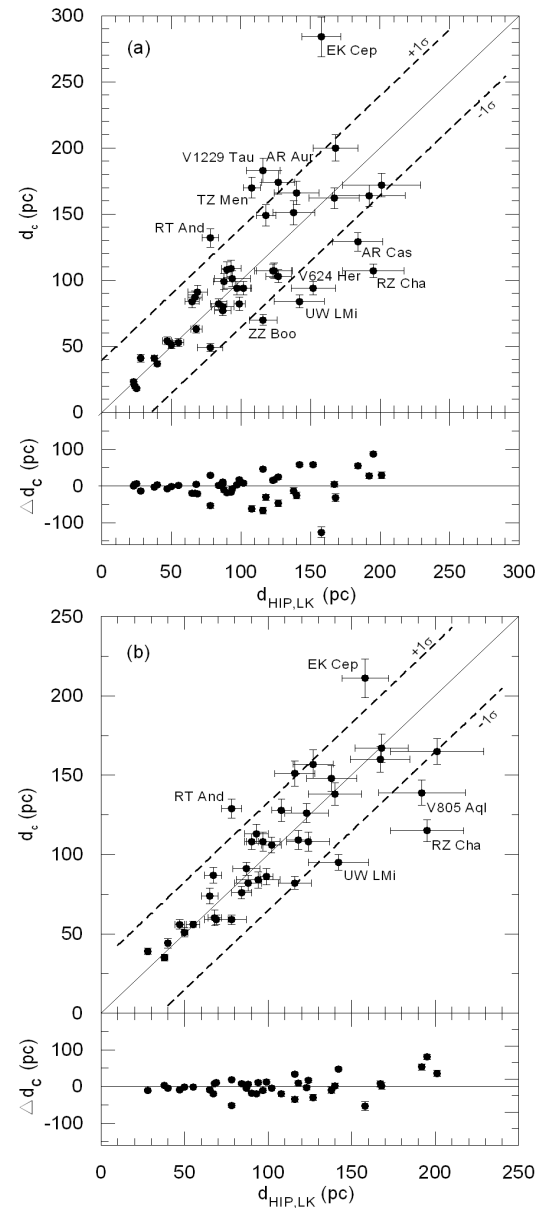


Fig. 3 Comparison of the distances calculated from LK corrected *Hipparcos* parallaxes with the predicted distances from Eqs. 5(a) and 6 (b).

5 Discussions and conclusions

We have suggested absolute magnitude calibrations for detached binaries based on LK corrected *Hipparcos* parallaxes. The calibration equations cover a wide range of colours and absolute magnitudes.

The distances of calibration stars were calculated using the absolute magnitudes obtained from the LCs relations and compared with the *Hipparcos* distances (Fig. 3). Although distances are in agreement in general (concentrated on diagonal), there is a considerable scatter for some systems. Large deviations from the LCs relations are mostly seen for the systems whose distances are higher than ~ 100 pc with the exception of RT And, which is closer than 100

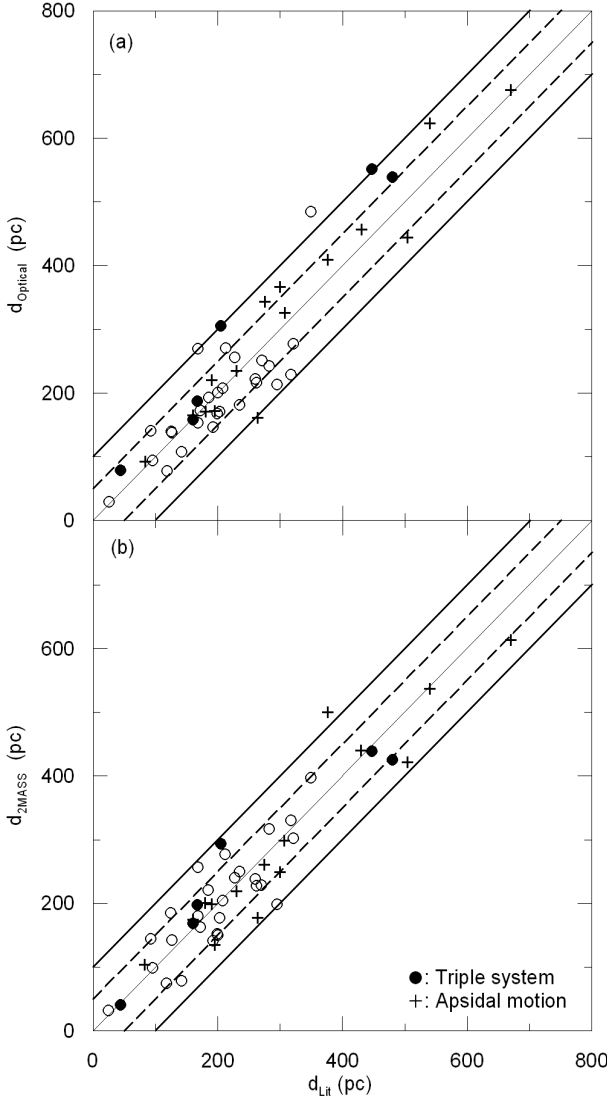


Fig. 4 The distances predicted from our LCs relations are compared to the distances used in literature, where various methods including trigonometric parallaxes were preferred. Stars with hypothetical third body or apsidal motion are indicated by different symbols. Vertical scale of (a) uses Eq. 5, while vertical axis of (b) uses Eq. 6. Thick-dashed and solid lines show 50 and 100 pc distances from the diagonal thin line representing equal values. Error bars are not shown for clarity.

pc. We have listed these scattered systems in Table 5. The table shows that distances from literature agree better with our distance estimates from the calibration relation including near-infrared colours. The table also indicates that *Hipparcos* distances are not in good agreement with the distances recorded in literature, in general, although their relative parallax errors are smaller than 0.15. One of the best examples is V1229 Tau. Southworth et al. (2005b) estimated the distance of V1229 Tau using three independent methods and found that *Hipparcos* distance is not in agreement with their results. Our estimates support Southworth et al.

Table 5 The distances of scattered stars in calibration sample obtained from various other sources in literature. Columns 2, 3 and 4 include distances calculated using calibration Eqs. 5, 6 and LK corrected *Hipparcos* parallaxes, respectively. Column 5 shows the distances collected from literature.

Star	Eq. 5 d (pc)	Eq. 6 d (pc)	Hip d_{LK} (pc)	Lit. d (pc)	Refs
RT And	132 \pm 7	129 \pm 6	78 \pm 6	103	(1)
V805 Aql	164 \pm 8	139 \pm 8	192 \pm 26	—	(–)
AR Aur	174 \pm 9	157 \pm 9	127 \pm 12	136 \pm 7	(2)
ZZ Boo	70 \pm 4	82 \pm 4	116 \pm 10	79	(3)
AR Cas	129 \pm 7	—	184 \pm 18	—	(–)
EK Cep	284 \pm 15	211 \pm 12	158 \pm 14	190	(4)
RZ Cha	107 \pm 5	115 \pm 7	195 \pm 22	190 \pm 10	(5)
V624 Her	94 \pm 5	—	152 \pm 16	111	(6)
UW LMi	84 \pm 5	95 \pm 5	141 \pm 18	82	(7)
TZ Men	170 \pm 8	128 \pm 7	108 \pm 6	120 \pm 10	(8)
V1229 Tau	183 \pm 9	151 \pm 8	116 \pm 12	139 \pm 4	(9)

(1) Arevalo et al. (1995), (2) Semeniuk (2000), (3) Popper (1998),

(4) Popper (1987), (5) Andersen et al. (1975), (6) Lacy (1979),

(7) Nordström et al. (2004), (8) Andersen et al. (1987), (9)

Southworth et al. (2005b)

(2005b), but not in agreement with *Hipparcos* distance. Thus, it seems that, in selecting stars for such calibration studies, not only relative parallax errors but also parallaxes higher than 10 mas must be carefully taken into account.

It has been found that the distances indicated by the LCs relations and various methods are in agreement (see Fig. 4). Although there is some scattering in the figure, almost all systems are located very near to the diagonal line representing equal values. It is interesting to note that the systems in Fig. 4 with third body or apsidal motion do not display larger scatter in comparison to other stars.

Normally, colour-magnitude relation exists for main-sequence single stars which is the main part of HR diagram itself. Similar colour-magnitude relation obviously exists also for main-sequence binaries with a deviation of about 0.50 mag (see Table 3). This could be explained by an argument that the greatest deviation from the relation of single star must occur when two components of the binary are identical. For such cases a binary system would appear 0.75 mag brighter than a single star. So, deviation of binary system cannot be higher than 0.75 mag on the brightness scale. In fact, deviation becomes smaller if one of the stars becomes cooler. When the cooler star's contribution becomes negligible, the system behaves as single star. Assuming that, we have various systems so that expected deviation would be about smaller than 0.40 mag on the brightness scale on an average. This limit is well within the standard deviation predicted in Table 3. Colour axis deviation from single stars are also expected to be negligible. Because at both limits colour of the system is like a single star. When two components were identical there would be no colour deviation. When the temperature difference between components increases sys-

tem colour approaches to the colour of the dominant component.

The results of this study will help to understand space distributions and evolution of detached binaries in the solar neighbourhood. Indirectly, it will help to improve information about single stars. We suggest that the LCs relations are useful statistical tools to calculate the distances of detached binaries from their optical and near-infrared observations since the LCs relations are based on the most reliable distance estimation method (trigonometric parallax). Distances calculated from the LCs relations can give clues for astrometric observations of these systems, as well. Finally, it should be noted that future astrometric observations of detached binaries such as *GAIA* and *SIM* missions, will refine the LCs and PLCs relations.

6 Acknowledgments

We would like to thank the anonymous referee for his useful and constructive comments concerning the manuscript. This work has been supported in part by the Scientific and Technological Research Council (TÜBİTAK) 106T688. This publication makes use of data products from the Two Micron All Sky Survey, which is a joint project of the University of Massachusetts and the Infrared Processing and Analysis Center/California Institute of Technology, funded by the National Aeronautics and Space Administration and the National Science Foundation. This research has made use of the SIMBAD database, operated at CDS, Strasbourg, France and NASA's Astrophysics Data System. Part of this work was supported by the Research Fund of the University of Istanbul, Project Number: BYP1379.

References

- Ak, T., Bilir, S., Ak, S., Retter, A.: 2007, NewA 12, 446
- Andersen, J.: 1975, A&A 45, 203
- Andersen, J., Gjerloff, H., Imbert, M.: 1975, A&A 44, 349
- Andersen, J., Vaz, L.P.R.: 1984, A&A 130, 102
- Andersen, J., Clausen, J.V., Nordström, B.: 1984, A&A 134, 147
- Andersen, J., Gimenez, A.: 1985, A&A 145, 206
- Andersen, J., Nordström, B., Garcia, J.M., Gimenez, A.: 1987, A&A 174, 107
- Andersen, J., Clausen, J.V., Nordström, B.: 1987, A&A 175, 60
- Andersen, J., Clausen, J.V., Magain, P.: 1989, A&A 211, 346
- Andersen, J.: 1991, A&ARv 3, 91
- Andersen, J., Clausen, J.V., Gimenez, A.: 1993, A&A 277, 439
- Arevalo, M.J., Lazaro, C., Claret, A.: 1995, AJ 110, 1376
- Bahcall, J.N., Soneira, R.M.: 1980, ApJS 44, 73
- Barembaum, M.J., Etzel, P.B.: 1995, AJ 109, 2680
- Bakış, V., Bakış, H., Eker, Z., Demircan, O.: 2007, MNRAS 382, 609
- Bakış, V., Bakış, H., Demircan, O., Eker, Z.: 2008, MNRAS 384, 1657
- Bilir, S., Güver, T., Aslan, M.: 2006, AN 327, 693
- Bilir, S., Ak, S., Karaali, S., Cabrera-Lavers, A., Chonis, T.S., Gaskell, C.M.: 2008, MNRAS 384, 1178
- Bozkurt, Z., Değirmenci, O.: 2007, MNRAS 379, 370
- Bulut, I., Demircan, O.: 2007, MNRAS 378, 179
- Clausen, J.V., Gyldenkerne, K., Gronbech, B.: 1976, A&AS 23, 261
- Clausen, J.V., Gimenez, A., Scarfe, C.: 1986, A&A 167, 287
- Clement, R., Garcia, M., Reglero, V., Suso, J., Fabregat, J.: 1997, A&AS 125, 529
- Clement, R., Reglero, V., Garcia, M., Fabregat, J., Suso, J.: 1997, A&AS 124, 499
- Covey, K.R., et al.: 2007, AJ 134, 2398
- Cox, A.N.: 2000, *Allen's astrophysical quantities*, 4th ed. Publisher: New York: AIP Press; Springer, 2000. Ed. by Arthur N. Cox. ISBN: 0387987460
- Cutispoto, G., Kuerster, M., Messina, S., Rodono, M., Tagliaferri, G.: 1997, A&A 320, 586
- Cutri, R.M., et al.: 2003, VizieR On-Line Data Catalog: II/246
- de Landtsheer, A.C., Mulder, P.S.: 1983, A&A 127, 297
- Debernardi, Y., North, P.: 2001, A&A 374, 204
- Değirmenci, O.L., Gülmén, O., Sezer, C., İbanoğlu, C., Çakırlı, O.: 2003, A&A 409, 959
- Demircan, O., Kaya, Y., Tüfekçioğlu, Z.: 1994, Ap&SS 222, 213
- Eker, Z., Ak, N. F., Bilir, S., Doğru, D., Tüysüz, M., Soydugan, E., Bakış, H., Uğraş, B., Soydugan, F., Erdem, A., Demircan, O.: 2008, MNRAS (in press), (astro/ph: 0805.4517)
- ESA: 1997, The Hipparcos and Tycho Catalogues, ESA SP-1200. ESA, Noordwijk
- Fiorucci, M., Munari, U.: 2003, A&A 401, 781
- Groenewegen, M.A.T., Decin, L., Salaris, M., De Cat, P.: 2007, A&A 463, 579
- Haefner, R., Skillen, I., de Groot, M.: 1987, A&A 179, 141
- Holmgren, D.E., Hadrava, P., Harmanec, P., Eenens, P., Corral, L.J., Yang, S., Ak, H., Bozic, H.: 1999, A&A 345, 855
- Jerzykiewicz, M.: 2001, AcA 51, 151
- Jorgensen, H.E.: 1979, A&A 72, 356
- Khodykin, S.A., Vedenev, V.G.: 1997, ApJ 475, 798
- Lacy, C.H.S.: 1979, ApJ 228, 817
- Lacy, C.H.S., Frueh, M.L.: 1985, ApJ 295, 569
- Lacy, C.H.S., Frueh, M.L.: 1987, AJ 94, 712
- Lacy, C.H.S.: 1997a, AJ 113, 1091
- Lacy, C.H.S.: 1997b, AJ 114, 2140
- Lacy, C.H.S., Torres, G., Latham, D.W., Zakirov, M.M., Arzumanyants, G.C.: 1997, AJ 114, 1206
- Lacy, C.H.S.: 2002, AJ 124, 1162
- Lacy, C.H.S., Torres, G., Claret, A., Sabby, J.A.: 2002, AJ 123, 1013
- Lacy, C.H.S., Torres, G., Claret, A., Vaz, L.P.R.: 2005, AJ 130, 2838

- Lacy, C.H.S., Torres, G., Claret, A., Menke, J.L.: 2006, AJ 131, 2664
- Lastennet, E., Valls-Gabaud, D., Lejeune, Th., Oblak, E.: 1999, A&A 349, 485
- Latham, D. W., Nordström, B., Andersen, J., Torres, G., Stefanik, R.P., Thaller, M., Bester, M.J.: 1996, A&A 314, 864
- Lutz, T. E., Kelker, D. H.: 1973, PASP 85, 573
- Maiz Apellániz, J.: 2005, Proceedings of the Gaia Symposium "The Three-Dimensional Universe with Gaia" (ESA SP-576). Held at the Observatoire de Paris-Meudon, 4-7 October 2004. Editors: C. Turon, K.S. O'Flaherty, M. A. C. Perryman, p.179
- Marshall, D.J., Robin, A.C., Reylé, C., Schultheis, M., Picaud, S.: 2006, A&A 453, 635
- Maloney, F.P., Guinan, E.F., Boyd, P.T.: 1989, AJ 98, 1800
- Mochnacki, S.W.: 1981, ApJ 245, 650
- Munari, U., Tomov, T., Zwitter, T., Milone, E.F., Kallrath, J., Marrese, P.M., Boschi, F., Prsa, A., Tomasella, L., Moro, D.: 2001, A&A 378, 477
- Nelson, R.H., 2004, IBVS 5535, 1
- Nordström, B., Johansen, K.T.: 1994a, A&A 282, 787
- Nordström, B., Johansen, K.T.: 1994b, A&A 291, 777
- Nordström, B., Mayor, M., Andersen, J., Holmberg, J., Pont, F., Jorgensen, B.R., Olsen, E.H., Udry, S., Mowlavi, N.: 2004, A&A 418, 989
- Paczyński, B., Szczygiel, D.M., Pilecki, B., Pojmański, G.: 2006, MNRAS 368, 1311
- Petrova, A.V., Orlov, V.V.: 1999, AJ 117, 587
- Popper, D.M.: 1968, ApJ 154, 191
- Popper, D.M.: 1980, ARA&A 18, 115
- Popper, D.M.: 1981, ApJ 244, 541
- Popper, D.M., Etzel, P.B.: 1981, AJ 86, 102
- Popper, D.M.: 1984, AJ 89, 1057
- Popper, D.M., Andersen, J., Clausen, J.V., Nordström, B.: 1985, AJ 90, 1324
- Popper, D.M., Lacy, C.H.S., Frueh, M.L., Turner, A.E.: 1986, AJ 91, 383
- Popper, D.M.: 1987, ApJ 313L, 81
- Popper, D.M.: 1998, PASP 110, 919
- Rucinski, S.M.: 1997, Mem. Soc. Astron. Ital 45, 799
- Rucinski, S.M.: 1994, PASP 106, 462
- Rucinski, S.M., Duerbeck, H.W.: 1997, PASP 109, 1340
- Rucinski, S.M.: 2004, NewAR 48, 703
- Schlegel, D.J., Finkbeiner, D.P., Davis, M.: 1998, ApJ 500, 525
- Semeniuk, I.: 2000, AcA 50, 381
- Smith, H.Jr.: 1987, A&A 171, 336
- Siviero, A., Munari, U., Sordo, R., Dallaporta, S., Marrese, P.M., Zwitter, T., Milone, E.F.: 2004, A&A 417, 1083
- Skrutskie, M.F., Cutri, R.M., Stiening, R., Weinberg, M.D., Schneider, S., et al.: 2006, AJ 131, 1163
- Southworth, J., Maxted, P.F.L., Smalley, B.: 2004, MNRAS 351, 1277
- Southworth, J., Smalley, B., Maxted, P.F.L., Claret, A., Etzel, P.B.: 2005a, MNRAS 363, 529
- Southworth, J., Maxted, P.F.L., Smalley, B.: 2005b, A&A 429, 645
- Srivastava, R.K.: 1987, Ap&SS 138, 197
- Torres, G., Lacy, C.H., Marschall, L.A., Sheets, H.A., Mader, J.A.: 2006, ApJ 640, 1018
- Vaz, L.P.R., Andersen, J.: 1984, A&A 132, 219